Assessment of DFT functionals for computing the dipole moment of endohedral complexes with PNO-LCCSD-F12/aug-cc-pVTZ as reference method

Justyna Kozłowska,[*,†] Max Schwilk,[*,‡,¶] Agnieszka Roztoczyńska,[†] and Wojciech Bartkowiak[†]

†*Department of Physical and Quantum Chemistry, Wrocław University of Science and Technology, Wybrzeże Wyspiańskiego 27, PL–50370 Wrocław, Poland*

‡*Department of Chemistry, University of Basel, Klingelbergstrasse 80, CH-4056 Basel, Switzerland*

¶*Institute for Theoretical Chemistry, University of Stuttgart, Pfaffenwaldring 55, D-70569 Stuttgart, Germany*

E-mail: justyna.kozlowska@pwr.edu.pl; max.schwilk@unibas.ch

Electronic Supporting Information

Table S1: Deviations in au of the PNO-LCCSD-F12A/B finite field response dipole moment with respect to canonical results for the molecules with 1–19 atoms of the FH set (80 molecules in total).
Tight PNO domains are defined as: `thrpno_en_cc`=0.997, `thrpno_occ_cc`=10^{-8}.
Default PNO domains are defined as: `thrpno_en_cc`=0.99, `thrpno_occ_cc`=10^{-7}.
CABS correction is included, basis set: VTZ-F12, DF basis: aug-cc-pVnZ. For further details on the canonical and local calculations see main text.
"SD": Standard deviation; "MAD": Mean absolute deviation; "MAXD": Maximum deviation; "NORM": deviation of the norm of the vector; "COMP": deviation of the compounds of the vector (along x, y, and z axis).

Tight PNO domains, QZ DF basis

		CCSD-F12A	CCSD-F12B
SD	NORM	0.00139	0.00143
	COMP	0.00130	0.00128
MAD	NORM	0.00075	0.00081
	COMP	0.00057	0.00059
MAXD	NORM	0.00578	0.00572
	COMP	0.01078	0.01027

Tight PNO domains, TZ DF basis

		CCSD-F12A	CCSD-F12B
SD	NORM	0.00144	0.00153
	COMP	0.00131	0.00133
MAD	NORM	0.00080	0.00088
	COMP	0.00060	0.00064
MAXD	NORM	0.00639	0.00628
	COMP	0.01118	0.01078

Default PNO domains, TZ DF basis

		CCSD-F12A	CCSD-F12B
SD	NORM	0.00130	0.00127
	COMP	0.00110	0.00102
MAD	NORM	0.00086	0.00085
	COMP	0.00063	0.00061
MAXD	NORM	0.00491	0.00508
	COMP	0.00501	0.00495

Table S2: Deviations in au of the PNO-LCCSD-F12A/B finite field response dipole moment for molecules with 20–39 atoms of the FH set (23 molecules in total). For the description see caption of Table (5).

Comparison to tight domains, QZ DF basis,
molecules with 20-29 atoms, 21 molecules in total

Tight PNO domains, TZ DF basis

		CCSD-F12A	CCSD-F12B
SD	NORM	0.00022	0.00022
	COMP	0.00021	0.00022
MAD	NORM	0.00016	0.00016
	COMP	0.00013	0.00014
MAXD	NORM	0.00057	0.00052
	COMP	0.00088	0.00098

Default PNO domains, TZ DF basis

		CCSD-F12A	CCSD-F12B
SD	NORM	0.00071	0.00089
	COMP	0.00056	0.00066
MAD	NORM	0.00043	0.00057
	COMP	0.00037	0.00044
MAXD	NORM	0.00229	0.00233
	COMP	0.00202	0.00227

Comparison to tight domains, QZ DF basis,
molecules with 30-39 atoms, 2 molecules in total

Tight PNO domains, TZ DF basis

		CCSD-F12A	CCSD-F12B
SD	NORM	0.00004	0.00005
	COMP	0.00009	0.00009
MAD	NORM	0.00004	0.00004
	COMP	0.00005	0.00004
MAXD	NORM	0.00006	0.00006
	COMP	0.00022	0.00021

Default PNO domains, TZ DF basis

		CCSD-F12A	CCSD-F12B
SD	NORM	0.00025	0.00033
	COMP	0.00023	0.00025
MAD	NORM	0.00019	0.00026
	COMP	0.00017	0.00019
MAXD	NORM	0.00035	0.00047
	COMP	0.00037	0.00049

Table S3: PNO-LCCSD-F12A/B finite field response dipole moment in au for the AB@CNT(n,n) complexes with tight and default PNO domains. The component along the main axis (z-axis), the norm, and the (artefact) components along the x and y axis are given. For the PNO domain threshold description see Table (5) and the main text. Basis set: VTZ-F12, DF basis: aug-cc-pVTZ.

LiF@CNT(3,3), tight PNO domains

		CCSD-F12A	CCSD-F12B	
X-COMP		0.000138	-0.000425	
Y-COMP		0.002494	0.002551	
Z-COMP		0.535080	0.535538	
NORM		0.535086	0.535544	

LiF@CNT(4,4), tight PNO domains

		CCSD-F12A	CCSD-F12B	
X-COMP		-0.000108	-0.000093	
Y-COMP		-0.000092	-0.000060	
Z-COMP		0.681957	0.682664	
NORM		0.681957	0.682664	

LiF@CNT(3,3), default PNO domains

	HF	CCSD-F12A	CCSD-F12B	MP2-F12
X-COMP	-0.000061	-0.002010	-0.004308	-0.007223
Y-COMP	0.000006	0.001525	0.001143	0.000260
Z-COMP	0.546206	0.539266	0.541635	0.425936
NORM	0.546206	0.539272	0.541654	0.425997

LiF@CNT(4,4), default PNO domains

	HF	CCSD-F12A	CCSD-F12B	MP2-F12
X-COMP	-0.000060	-0.000098	-0.000103	-0.000070
Y-COMP	-0.000054	-0.000130	-0.000100	-0.000125
Z-COMP	0.729585	0.687699	0.689753	0.579729
NORM	0.729585	0.687699	0.689753	0.579729

LiF@CNT(5,5), default PNO domains

	HF	CCSD-F12A	CCSD-F12B	MP2-F12
X-COMP	-0.000053	-0.004653	-0.006468	-0.006382
Y-COMP	0.000020	0.001858	0.004473	0.006194
Z-COMP	0.886569	0.832724	0.833004	0.747361
NORM	0.886569	0.832739	0.833042	0.747414

Table S4: The values of the electric dipole moment (μ_z) of the LiF@CNT(n,n) complexes (with n=3,4,5), predicted by various DFT functionals as well as the HF, MP2, and PNO-LCCSD-F12 methods (in au). The **% error** was calculated with respect to the PNO-LCCSD-F12/aug-cc-pVTZ results. The methods for which **|% error| ≤ 7%** are highlighted in orange (underestimated dipole moment w.ṙ. t. the reference) or gray (overestimated dipole moment w.ṙ. t. the reference). The values of μ_z were computed using the aug-cc-pVTZ basis set. Due to numerical instabilities the value of μ_z could not be determined for LiF@CNT(5,5) using the LC-N12 functional.

LiF@CNT(3,3)			LiF@CNT(4,4)			LiF@CNT(5,5)		
method	μ_z	**% error**	**method**	μ_z	**% error**	**method**	μ_z	**% error**
B3LYP	0.415	-22.7	B3LYP	0.574	-16.0	B3LYP	0.737	-11.7
B3PW91	0.416	-22.5	B3PW91	0.572	-16.3	B3PW91	0.738	-11.6
B97-2	0.418	-22.2	B97-2	0.576	-15.7	B97-2	0.742	-11.1
B97D	0.374	-30.4	B97D	0.528	-22.7	B97D	0.692	-17.1
BLYP	0.372	-30.7	BLYP	0.526	-23.0	BLYP	0.687	-17.7
BMK	0.464	-13.6	BMK	0.632	-7.5	BMK	0.784	-6.1
CAM-B3LYP	0.468	-12.8	CAM-B3LYP	0.630	-7.8	CAM-B3LYP	0.789	-5.5
HCTH	0.371	-30.9	HCTH	0.532	-22.1	HCTH	0.703	-15.8
HISS	0.449	-16.4	HISS	0.610	-10.7	HISS	0.774	-7.3
HSE06	0.421	-21.6	HSE06	0.575	-15.8	HSE06	0.740	-11.4
LC-BLYP	0.523	-2.6	LC-BLYP	0.691	1.2	LC-BLYP	0.845	1.2
LC-HCTH	0.522	-2.8	LC-HCTH	0.702	2.8	LC-HCTH	0.703	-15.8
LC-N12	0.528	-1.7	LC-N12	0.695	1.8	LC-N12	–	–
LC-revTPSS	0.524	-2.4	LC-revTPSS	0.688	0.7	LC-revTPSS	0.846	1.3
LC-τHCTH	0.527	-1.9	LC-τHCTH	0.706	3.4	LC-τHCTH	0.844	1.1
LSDA	0.374	-30.4	LSDA	0.520	-23.9	LSDA	0.680	-18.6
M06	0.408	-24.0	M06	0.588	-13.9	M06	0.727	-12.9
M06-2X	0.488	-9.1	M06-2X	0.635	-7.0	M06-2X	0.783	-6.2
M06-HF	0.564	5.0	M06-HF	0.682	-0.1	M06-HF	0.822	-1.6
M06L	0.387	-27.9	M06L	0.561	-17.9	M06L	0.720	-13.8
M11	0.521	-3.0	M11	0.661	-3.2	M11	0.808	-3.2
M11-L	0.370	-31.1	M11-L	0.519	-24.0	M11-L	0.672	-19.5
MN12-L	0.390	-27.4	MN12-L	0.544	-20.4	MN12-L	0.696	-16.6
MN12-SX	0.417	-22.3	MN12-SX	0.573	-16.1	MN12-SX	0.724	-13.3
mPW1PW91	0.425	-20.9	mPW1PW91	0.581	-14.9	mPW1PW91	0.747	-10.5
N12	0.364	-32.2	N12	0.522	-23.6	N12	0.694	-16.9
N12-SX	0.415	-22.7	N12-SX	0.581	-14.9	N12-SX	0.749	-10.3
PBE	0.371	-30.9	PBE	0.522	-23.6	PBE	0.686	-17.8
PBE0	0.425	-20.9	PBE0	0.581	-14.9	PBE0	0.746	-10.7
revTPSS	0.376	-30.0	revTPSS	0.530	-22.4	revTPSS	0.697	-16.5
SOGGA11-X	0.457	-14.9	SOGGA11-X	0.619	-9.4	SOGGA11-X	0.768	-8.0
τHCTH	0.369	-31.3	τHCTH	0.524	-23.3	τHCTH	0.693	-17.0
τHCTHHYB	0.406	-24.4	τHCTHHYB	0.560	-18.0	τHCTHHYB	0.723	-13.4
TPSSH	0.397	-26.1	TPSSH	0.552	-19.2	TPSSH	0.720	-13.8
ωB97	0.513	-4.5	ωB97	0.684	0.1	ωB97	0.829	-0.7
ωB97X	0.499	-7.1	ωB97X	0.669	- 2.0	ωB97X	0.820	-1.8
ωB97X-D	0.475	-11.5	ωB97X-D	0.639	-6.4	ωB97X-D	0.795	-4.8
HF	0.546	1.7	HF	0.730	6.9	HF	0.887	6.2
MP2	0.430	-19.9	MP2	0.588	-13.9	MP2	0.752	-9.9
LCCSD-F12	0.537	0.0	LCCSD-F12	0.683	0.0	LCCSD-F12	0.835	0.0

Table S5: The values of the electric dipole moment (μ_z) of the HCl@CNT(n,n) complexes (with n=3,4,5), predicted by various DFT functionals as well as the HF, MP2 and PNO-LCCSD-F12 methods (in au). The **% error** was calculated with respect to the PNO-LCCSD-F12/aug-cc-pVTZ results. The methods for which **|% error| ≤ 7%** are highlighted in orange (underestimated dipole moment w.r. t. the reference) or gray (overestimated dipole moment w.r. t. the reference). The values of μ_z were computed using the aug-cc-pVTZ basis set.

HCl@CNT(3,3)			HCl@CNT(4,4)			HCl@CNT(5,5)		
method	μ_z	**% error**	**method**	μ_z	**% error**	**method**	μ_z	**% error**
B4LYP	-0.554	20.2	B3LYP	0.017	-71.7	B3LYP	0.106	-14.5
B3PW91	-0.562	21.9	B3PW91	0.020	-66.7	B3PW91	0.109	-12.1
B97-2	-0.558	21.0	B97-2	0.023	-61.7	B97-2	0.110	-11.3
B97D	-0.585	26.9	B97D	0.005	-91.7	B97D	0.096	-22.6
BLYP	-0.588	27.5	BLYP	-0.002	-103.3	BLYP	0.092	-25.8
BMK	-0.527	14.3	BMK	0.046	-23.3	BMK	0.125	0.8
CAM-B3LYP	-0.488	5.9	CAM-B3LYP	0.043	-28.3	CAM-B3LYP	0.121	-2.4
HCTH	-0.578	25.4	HCTH	0.010	-83.3	HCTH	0.101	-18.5
HISS	-0.540	17.1	HISS	0.036	-40.0	HISS	0.121	-2.4
HSE06	-0.563	22.1	HSE06	0.021	-65.0	HSE06	0.110	-11.3
LC-BLYP	-0.417	-9.5	LC-BLYP	0.075	25.0	LC-BLYP	0.142	14.5
LC-HCTH	-0.392	-15.0	LC-HCTH	0.076	26.7	LC-HCTH	0.143	15.3
LC-N12	-0.405	-12.1	LC-N12	0.085	41.7	LC-N12	0.150	21.0
LC-revTPSS	-0.437	-5.2	LC-revTPSS	0.076	26.7	LC-revTPSS	0.143	15.3
LC-τHCTH	-0.390	-15.4	LC-τHCTH	0.075	25.0	LC-τHCTH	0.142	14.5
LSDA	-0.590	28.0	LSDA	0.007	-88.3	LSDA	0.104	-16.1
M06	-0.532	15.4	M06	0.039	-35.0	M06	0.115	-7.3
M06-2X	-0.489	6.1	M06-2X	0.051	-15.0	M06-2X	0.123	-0.8
M06-HF	-0.433	-6.1	M06-HF	0.078	30.0	M06-HF	0.138	11.3
M06L	-0.586	27.1	M06L	0.018	-70.0	M06L	0.109	-12.1
M11	-0.441	-4.3	M11	0.066	10.0	M11	0.130	4.8
M11-L	-0.519	12.6	M11-L	0.013	-78.3	M11-L	0.095	-23.4
MN12-L	-0.608	31.9	MN12-L	0.021	-65.0	MN12-L	0.110	-11.3
MN12-SX	-0.560	21.5	MN12-SX	0.026	-56.7	MN12-SX	0.110	-11.3
mPW1PW91	-0.557	20.8	mPW1PW91	0.024	-60.0	mPW1PW91	0.112	-9.7
N12	-0.594	28.9	N12	0.008	-86.7	N12	0.103	-16.9
N12-SX	-0.569	23.4	N12-SX	0.026	-56.7	N12-SX	0.115	-7.3
PBE	-0.598	29.7	PBE	0.002	-96.7	PBE	0.097	-21.8
PBE0	-0.558	21.0	PBE0	0.024	-60.0	PBE0	0.112	-9.7
revTPSS	-0.623	35.1	revTPSS	0.000	-100.0	revTPSS	0.097	-21.8
SOGGA11-X	-0.534	15.8	SOGGA11-X	0.038	-36.7	SOGGA11-X	0.119	-4.0
τHCTH	-0.587	27.3	τHCTH	0.006	-90.0	τHCTH	0.098	-21.0
τHCTHHYB	-0.569	23.4	τHCTHHYB	0.017	-71.7	τHCTHHYB	0.106	-14.5
TPSSH	-0.594	28.9	TPSSH	0.010	-83.3	TPSSH	0.104	-16.1
ωB97	-0.430	-6.7	ωB97	0.073	21.7	ωB97	0.137	10.5
ωB97X	-0.452	-2.0	ωB97X	0.062	3.3	ωB97X	0.131	5.6
ωB97X-D	-0.490	6.3	ωB97X-D	0.048	-20.0	ωB97X-D	0.124	0.0
HF	-0.449	-2.6	HF	0.076	26.7	HF	0.143	15.3
MP2	-0.644	39.7	MP2	0.015	-75.0	MP2	0.109	-12.1
LCCSD-F12	-0.461	0.0	LCCSD-F12	0.060	0.0	LCCSD-F12	0.124	0.0

Table S6: The difference between absolute values of **% error** obtained for aug-cc-pVTZ and aug-cc-pVDZ/cc-pVTZ/6-31++G(d,p) in the case of LiF@CNT(n,n) complexes (with n=3,4,5). The **% error** was calculated with respect to the PNO-LCCSD-F12/aug-cc-pVTZ results. Negative values of determined differences denote that the DFT method with the aug-cc-pVTZ basis set is closer to the reference than with the basis set with which it is compared. Analogously, positive values of determined differences denote that the DFT method with the aug-cc-pVTZ basis set is less closer to the reference than the basis set with which it is compared.

	% error: aug-cc-pVTZ vs. aug-cc-pVDZ			% error: aug-cc-pVTZ vs. cc-pVTZ			% error: aug-cc-pVTZ vs. 6-31++G(d,p)		
LiF@:	CNT(3,3)	CNT(4,4)	CNT(5,5)	CNT(3,3)	CNT(4,4)	CNT(5,5)	CNT(3,3)	CNT(4,4)	CNT(5,5)
B3LYP	0.1	0.3	0.4	-5.0	-4.6	-3.4	-2.5	0.1	-0.5
B3PW91	0.3	0.5	0.6	-3.8	-3.8	-3.1	-2.4	0.3	-0.3
B97-2	0.3	0.5	0.6	-4.5	-4.1	-3.2	-2.5	0.3	-0.2
B97D	0.5	0.7	0.6	-5.4	-4.7	-3.6	-2.5	0.5	-0.5
BLYP	0.2	0.3	0.5	-6.0	-5.1	-3.8	-2.6	0.2	-0.9
BMK	-0.3	0.3	0.7	-4.3	-4.0	-2.7	-2.3	-0.3	-0.5
CAM-B3LYP	0.1	0.2	0.4	-4.4	-4.3	-3.3	-2.2	0.1	-0.2
HCTH	-0.5	0.0	0.3	-7.7	-5.8	-4.0	-2.7	-0.5	-0.8
HISS	0.3	0.4	0.4	-3.3	-3.5	-2.9	-2.2	0.3	0.0
HSE06	0.3	0.4	0.4	-4.3	-4.0	-3.2	-2.4	0.3	-0.4
LC-BLYP	0.1	-0.1	-0.3	-3.4	-3.7	-0.8	0.7	0.1	-0.2
LC-HCTH	-0.6	0.4	13.2	-7.2	-5.8	14.1	1.9	-0.6	13.3
LC-N12	1.6	-1.0	0.0	-0.3	-1.5	0.0	1.7	1.6	0.0
LC-revTPSS	0.3	-0.3	-0.4	-2.3	-2.8	-0.2	-0.2	0.3	-0.5
LC-τHCTH	-1.0	0.2	-0.4	-7.1	-5.8	-1.6	2.1	-1.0	-0.1
LSDA	0.2	0.2	0.4	-4.2	-4.1	-3.4	-2.3	0.2	-0.9
M06	-0.7	-0.1	0.9	-2.7	-3.6	-2.9	-2.9	-0.7	0.0
M06-2X	-0.7	-0.3	-0.3	-3.1	-2.8	-2.5	-2.7	-0.7	-0.6
M06-HF	-1.3	-0.5	0.3	0.4	-1.2	-1.4	-1.1	-1.3	1.2
M06L	-0.5	-0.2	0.1	-1.6	-2.7	-3.3	-2.8	-0.5	-0.5
M11	2.7	1.8	1.0	-33.2	-1.5	-2.6	-0.6	2.7	1.6
M11-L	-0.6	1.2	1.6	-5.1	-4.2	-2.9	-2.4	-0.6	0.8
MN12-L	0.9	2.2	1.7	-2.2	-1.6	-2.8	-1.0	0.9	1.0
MN12-SX	0.9	1.4	1.4	4.1	-3.2	-3.3	-1.8	0.9	0.9
mPW1PW91	0.5	0.6	0.5	-3.8	-3.8	-3.2	-2.4	0.5	-0.2
N12	0.7	0.5	0.3	-5.4	-4.5	-3.5	-2.8	0.7	-0.8
N12-SX	0.1	0.4	0.6	-4.1	-4.0	-2.9	-2.5	0.1	-0.3
PBE	0.3	0.4	0.5	-5.4	-4.7	-3.7	-2.6	0.3	-0.8
PBE0	0.2	0.4	0.4	-4.3	-4.1	-3.2	-2.4	0.2	-0.3
revTPSS	0.6	0.5	1.8	-4.1	-3.9	-2.0	-2.4	0.6	0.8
SOGGA11-X	0.0	1.0	1.4	-4.2	-3.9	-2.8	-2.2	0.0	0.7
τHCTH	0.9	0.9	0.7	-4.9	-4.4	-3.5	-2.3	0.9	-0.3
τHCTHHYB	0.7	0.6	0.5	-4.2	-4.0	-3.2	-2.3	0.7	-0.3
TPSSH	0.6	0.5	0.5	-3.9	-3.8	-3.2	-2.4	0.6	-0.4
ωB97	0.3	-0.4	0.5	-4.9	-4.1	-3.1	-1.7	0.3	0.3
ωB97X	-0.1	0.2	0.5	-5.0	-4.4	-3.2	-2.2	-0.1	0.1
ωB97X-D	0.1	0.4	0.6	-4.2	-4.0	-3.1	-2.2	0.1	0.1
HF	0.4	0.0	-0.4	-0.2	-4.0	2.8	2.5	0.4	-0.5
MP2	0.2	0.1	0.3	12.8	-2.0	-4.1	0.2	0.3	1.2

Table S7: The difference between absolute values of **% error** obtained for aug-cc-pVTZ and aug-cc-pVDZ/cc-pVTZ/6-31++G(d,p) in the case of HCl@CNT(n,n) complexes (with n=3,4,5). The **% error** was calculated with respect to the PNO-LCCSD-F12/aug-cc-pVTZ results. Negative values of determined differences denote that the DFT method with the aug-cc-pVTZ basis set is closer to the reference than with the basis set with which it is compared. Analogously, positive values of determined differences denote that the DFT method with the aug-cc-pVTZ basis set is less closer to the reference than the basis set with which it is compared.

	% error: aug-cc-pVTZ vs. aug-cc-pVDZ			% error: aug-cc-pVTZ vs. cc-pVTZ			% error: aug-cc-pVTZ vs. 6-31++G(d,p)		
HCl@:	CNT(3,3)	CNT(4,4)	CNT(5,5)	CNT(3,3)	CNT(4,4)	CNT(5,5)	CNT(3,3)	CNT(4,4)	CNT(5,5)
B3LYP	0.6	4.7	1.9	-2.7	-1.5	0.6	1.5	13.0	9.3
B3PW91	1.0	4.1	1.5	-2.4	-0.8	1.8	2.4	16.4	10.1
B97-2	1.0	3.9	1.4	-2.4	-2.0	0.8	2.3	16.7	10.4
B97D	0.7	4.5	1.5	-2.5	-2.8	0.5	1.4	13.6	9.1
BLYP	0.4	4.5	1.9	-2.8	-0.5	0.5	0.9	10.8	8.1
BMK	0.9	1.5	-3.5	-1.2	-11.5	0.2	2.1	13.5	-9.6
CAM-B3LYP	0.6	5.2	1.6	-2.4	-2.6	0.8	1.9	14.5	-7.2
HCTH	0.8	4.9	1.5	-3.1	-0.1	-2.4	2.2	17.8	11.1
HISS	1.2	5.0	1.7	-2.9	-0.8	1.9	2.9	18.2	-6.5
HSE06	1.0	4.7	1.4	-2.8	-0.8	1.6	2.5	17.4	10.5
LC-BLYP	-0.6	-6.0	-2.8	2.2	2.8	-1.2	-2.4	-16.0	-12.8
LC-HCTH	1.1	-6.3	-2.9	2.2	6.4	4.4	-1.5	-12.4	-12.6
LC-N12	-1.2	-10.2	-2.8	1.7	2.5	-7.7	-3.6	-16.2	-11.6
LC-revTPSS	-1.5	-5.6	-2.2	2.0	1.6	-2.6	-3.9	-22.0	-13.8
LC-τHCTH	1.6	-3.3	-4.5	2.1	13.8	5.7	0.1	-6.3	-12.8
LSDA	0.5	4.0	1.3	-2.3	-0.3	2.5	1.6	16.4	9.7
M06	0.1	3.3	1.0	-1.3	-20.7	-0.8	1.2	9.5	6.2
M06-2X	3.0	3.5	-1.3	-2.7	-13.4	-1.0	4.1	14.7	-10.8
M06-HF	-5.8	-7.3	-0.8	3.1	8.1	-4.7	-8.4	-26.5	-16.8
M06L	0.7	0.7	3.2	-0.5	-15.0	1.7	0.2	6.0	9.8
M11	-3.0	-11.2	-2.1	2.8	7.1	-5.7	-4.6	-16.1	-12.1
M11-L	-0.1	3.5	4.8	-3.1	-15.1	-2.6	-5.3	7.1	6.5
MN12-L	2.7	4.1	2.4	-1.8	-18.9	4.7	1.3	8.2	4.6
MN12-SX	2.9	2.7	3.0	-2.1	-10.2	1.1	1.4	8.4	7.5
mPW1PW91	1.2	3.9	1.5	-2.5	-0.3	1.8	2.5	17.1	9.4
N12	1.2	4.6	1.7	-1.5	3.3	2.3	2.1	13.7	8.0
N12-SX	1.4	3.0	1.8	-1.8	0.1	1.0	2.7	15.0	5.4
PBE	1.0	4.3	1.2	-2.6	0.4	1.0	1.9	15.8	9.3
PBE0	1.2	4.2	1.4	-2.6	-0.6	1.2	2.6	18.2	8.0
revTPSS	2.1	4.7	0.9	-2.7	2.9	2.7	3.1	16.4	8.3
SOGGA11-X	0.1	2.0	1.6	-1.8	-11.2	-0.5	1.4	14.5	-0.6
τHCTH	0.8	4.3	1.0	-2.7	-0.8	0.4	1.7	14.3	9.5
τHCTHHYB	0.7	4.2	1.4	-2.5	-2.8	1.6	1.8	14.8	9.9
TPSSH	1.9	4.3	0.9	-2.8	2.6	2.3	2.9	16.4	9.4
ωB97	-0.3	-4.4	-1.8	1.0	14.9	0.7	-2.7	-16.0	-11.9
ωB97X	3.8	-4.5	-1.7	5.9	-4.2	0.7	1.6	-15.8	-12.0
ωB97X-D	0.8	4.3	-1.2	-2.0	-7.9	-0.7	2.8	15.4	-10.8
HF	-2.3	-8.1	-3.3	2.3	2.2	-0.6	-4.0	-22.6	-13.1
MP2	0.9	0.3	2.1	-45.4	-7.9	0.3	6.4	20.9	-32.3

Table S8: The longitudinal components of electric dipole moment (μ_z) the isolated LiF or HCl molecule, predicted by various DFT functionals as well as HF, MP2 and LCCSD-F12 methods (in au).

	μ_z	
method	**LiF**	**HCl**
B3LYP	2.436	0.435
B3PW91	2.436	0.442
B97-2	2.447	0.442
B97D	2.451	0.428
BLYP	2.419	0.420
BMK	2.395	0.459
CAM-B3LYP	2.499	0.449
HCTH	2.447	0.435
HISS	2.410	0.459
HSE06	2.473	0.444
LC-BLYP	2.445	0.471
LC-HCTH	2.458	0.470
LC-N12	–	0.490
LC-revTPSS	2.469	0.472
LC-τHCTH	2.471	0.468
LSDA	2.398	0.445
M06	2.459	0.427
M06-2X	2.478	0.443
M06-HF	2.472	0.438
M06L	2.468	0.439
M11	2.465	0.446
M11-L	2.451	0.414
MN12-L	2.469	0.465
MN12-SX	2.467	0.440
mPW1PW91	2.451	0.444
N12	2.421	0.449
N12-SX	2.468	0.454
PBE	2.397	0.429
PBE0	2.447	0.446
revTPSS	2.411	0.428
SOGGA11-X	2.465	0.444
τHCTH	2.412	0.433
τHCTHHYB	2.439	0.439
TPSSH	2.428	0.438
ωB97	2.468	0.460
ωB97X	2.477	0.454
ωB97X-D	2.475	0.448
HF	2.542	0.472
MP2	2.479	0.439
LCCSD-F12	2.497	0.443

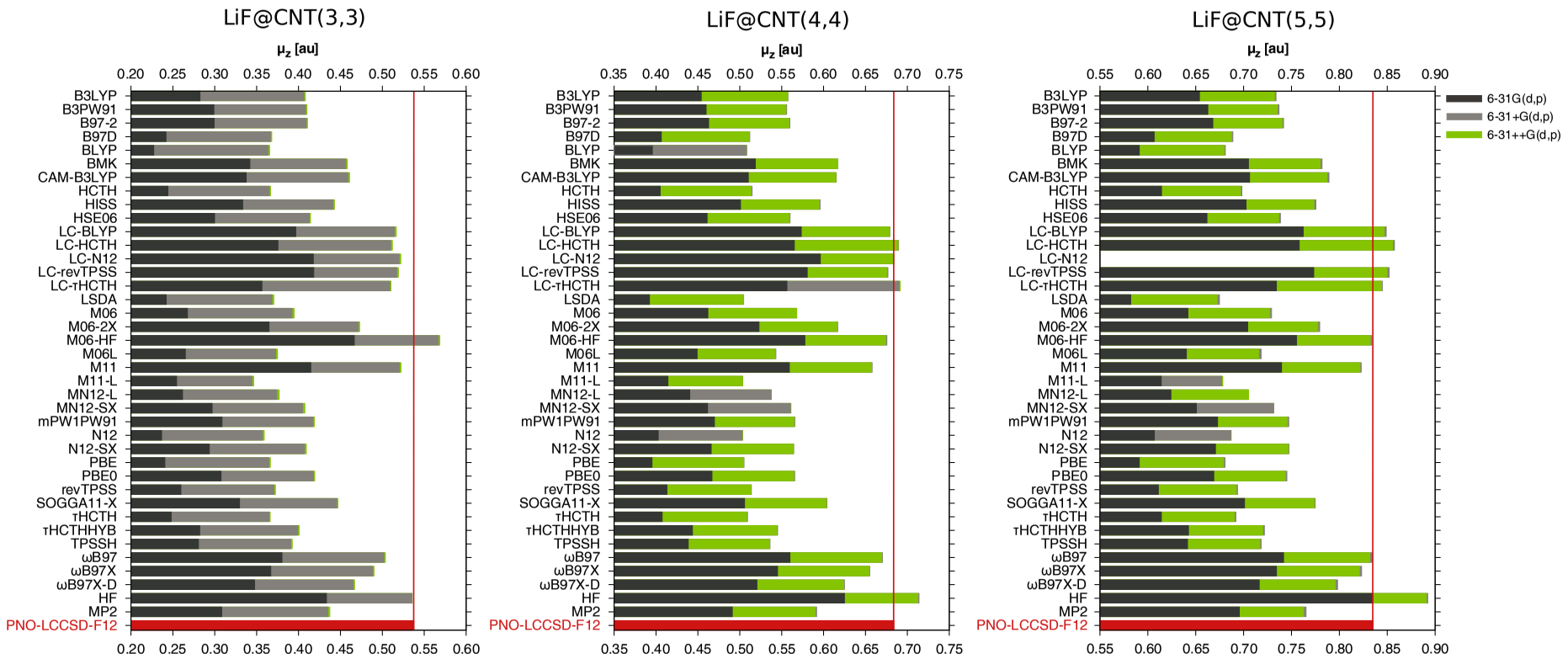

Figure S1: The static electric dipole moment (μ_z) of the LiF@CNT(n,n) complexes calculated using the 6-31G(d,p), 6-31+G(d,p), and 6-31++G(d,p) basis sets at different levels of DFT approximations. The reference PNO-LCCSD-F12 value of μ_z was computed using the aug-cc-pVTZ basis set.

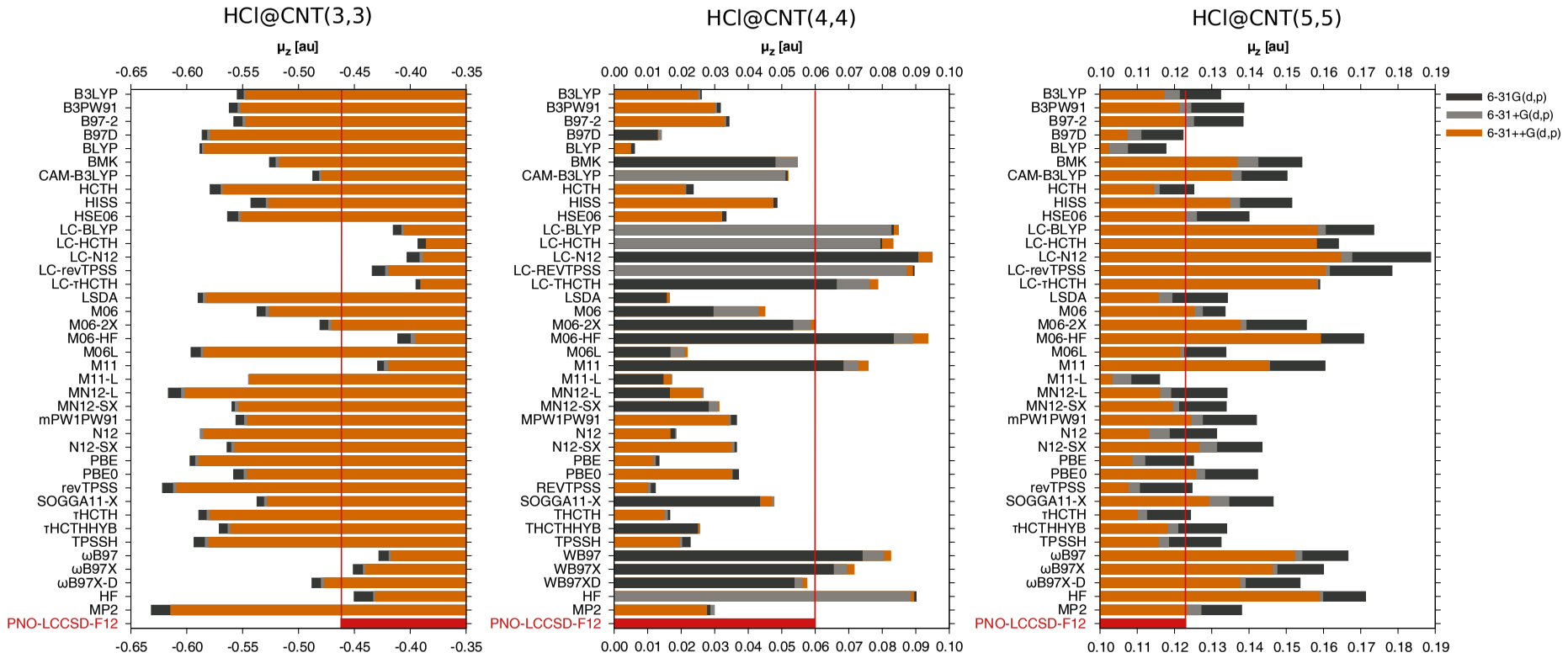

Figure S2: The static electric dipole moment (μ_z) of the HCl@CNT(n,n) complexes calculated using the 6-31G(d,p), 6-31+G(d,p), and 6-31++G(d,p) basis sets at different levels of DFT approximation. The reference PNO-LCCSD-F12 value of μ_z was computed using the aug-cc-pVTZ basis set.